

UVIT observations of UV-Bright stars in four Galactic Globular Clusters

Ranjan Kumar¹, Ananta C. Pradhan¹, M. Parthasarathy², Devendra K. Ojha³, Abhisek Mohapatra¹ and Jayant Murthy²

¹Dept. of Physics and Astronomy, National Institute of Technology, Rourkela - 769 008, India
email: ranjankmr488@gmail.com

²Indian Institute of Astrophysics, Bangalore - 560 034, India

³Dept. of Astronomy and Astrophysics, Tata Institute of Fundamental Research (TIFR), Mumbai - 400 005, India

Abstract. We have performed photometric analysis of four Galactic globular clusters (GGCs): NGC 4147, NGC 4590, NGC 5053 and NGC 7492 using far-UV and near-UV filters of the Ultraviolet Imaging Telescope (UVIT) on-board AstroSat. With the help of color-magnitude diagrams (CMDs), we have identified ~ 150 blue horizontal branch stars (BHBs), and ~ 40 blue straggler stars (BSS) in the four GGCs. We study the temperature and radial distribution of BHBs and BSS for the four GGCs.

Keywords. globular clusters: individual (NGC 4147, NGC 4590, NGC 5053 and NGC 7492), stars: horizontal-branch, techniques: photometric

1. Introduction

The ultraviolet (UV) light in old stellar populations of Galactic globular clusters (GGCs) is dominated by hot stars, such as blue horizontal branch stars (BHBs), blue hook stars (BHk), extreme blue horizontal branch stars (eBHBs), blue straggler stars (BSS), post asymptotic giant branch stars (pAGB) and hot sub-dwarfs (sdB, sdO) (Rood *et al.* 1998). UV emission is strongly dependent on the source temperature, therefore hot BHBs, among others are the strongest contributors to the far-UV flux of GGCs. Far-UV colors are well co-related with horizontal branch morphology in GGCs and have been studied vastly using Hubble Space Telescope (HST), Galaxy Evolution Explorer (GALEX) and Ultraviolet Imaging Telescope (UVIT) observations (see Schiavon *et al.* 2012; Dalessandro *et al.* 2012; Lagioia *et al.* 2015; Piotto *et al.* 2015; Milone *et al.* 2015; Subramaniam *et al.* 2017; Sahu *et al.* 2019). GGCs in halo region of Milky Way are less crowded in UV and hence, their observation in UV regime allows one to probe and separate out the bright stars effectively. Schiavon *et al.* (2012) have presented UV CMDs of 44 GGCs using GALEX observations and Piotto *et al.* (2015) have done the same for 58 GGCs from HST observations. The relative contributions of the various types of stars and the factors that might lead to larger or smaller populations of UV-Bright stars have remained an open question (Greggio & Renzini 1990; Dorman *et al.* 1995; Lee *et al.* 2002; Ambika *et al.* 2004; Jasniewicz *et al.* 2004; Sohn *et al.* 2006; Dalessandro *et al.* 2012). We present UV photometric study of four GGCs: NGC 4147, NGC 4590, NGC 5053 and NGC 7492 with the observations taken from UVIT on-board AstroSat (Tandon *et al.* 2017).

2. Observation and Data Reduction

The UVIT on-board AstroSat is performing observations in FUV (130–180 nm) and NUV (200–300 nm) bands, each having five filters with resolutions better than $1.8''$ since

Table 1. UVIT observation log of four GGCs.

Telescope		FUV			NUV		
Filter Name	λ_{eff} of filters (in Å)	BaF ₂ 1541	Sapphire 1608	Silica 1717	NUVB15 2196	NUVB13 2447	NUVB4 2632
Cluster Name (<i>gl</i> , <i>gb</i>) in degrees					Exposure Time in seconds		
NGC 4147	(252.85°, 77.19°)	1536	1648	1209	—	—	—
NGC 4590	(299.62°, 36.05°)	860	—	1406	1221	1739	1607
NGC 5053	(335.70°, 78.95°)	—	1423	217	—	1503	817
NGC 7492	(53.39°, -63.48°)	—	—	850	—	3276	3014

Table 2. Cluster parameters of GGCs and extracted UV-Bright sources from CMDs.

GGCs	Cluster parameters of GGCs						Number of UV-Bright sources					
	Gal. lat. in degree	Metallicity [Fe/H]	Distance (kpc)	E(B-V) (mag)	age (Gyr)	BHBs		BSS		eBHB		
						FUV	NUV	FUV	NUV			
NGC 7492	-63.48°	-1.80	26.3	0.0310	12.0	28	28	5	5	—	—	
NGC 5053	78.95°	-2.27	17.4	0.0149	12.3	25	35	2	29	1	—	
NGC 4590	36.05°	-2.23	10.3	0.0523	12.5	57	97	3	7	—	—	
NGC 4147	77.19°	-1.80	19.3	0.0221	13.5	34	—	4	—	—	—	

its launch in 2015 (Tandon *et al.* 2017). We have observed four GGCs, NGC 4147, NGC 4590, NGC 5053 and NGC 7492, using both the FUV and NUV filters of UVIT. The observational details are given in Table 1. We reduced the data and produced good quality images of the clusters using a customized software package CCIDLAB (Postma & Leahy 2017). We performed the crowded field photometry on the images using DAOPHOT package (Stetson 1987) available in IRAF. We have done the interstellar extinction correction on observed sources using Cardelli *et al.* (1989) extinction law considering E(B-V) value for each cluster from Schlegel *et al.* (1998) extinction map (see Table 2). We considered sources with AB magnitude limit up to 22.5 and 23.0 in FUV and NUV, respectively. We cross-matched the UVIT observed sources with GAIA DR2 catalogue (Gaia Collaboration *et al.* 2018) to get proper motion (PMRA, PMDEC) of observed sources. We separated out the cluster members from the field stars by selecting 1σ Gaussian distribution from mean PMRA and PMDEC as cluster members. The number of sources we obtained in FUV (NUV) as cluster members for GGCs, NGC 4590, NGC 5053, and NGC 7492 are 71(1875), 30(539) and 29(178), respectively. Since NGC 4147 has observation only with FUV filters, we could extract 45 cluster members in the FUV band.

3. Color Magnitude Diagram

After getting the catalog of sources for each cluster we have classified various stellar populations by plotting CMDs using various FUV, NUV and optical filters. We have shown the CMD, FUV(BaF₂) - NUV(B4) vs FUV(BaF₂) (Fig. 1(a)), and CMD, NUV(B4) - Gaia (G) vs NUV(B4) (Fig. 1(b)), for one of the clusters NGC 4590. The stellar populations present in the cluster were separated by identifying their various regions in the UV CMDs previously suggested by Schiavon *et al.* (2012); Subramaniam *et al.* (2017); Sahu *et al.* (2019). We can see that in FUV only BHBs and BSS are visible (Fig. 1(a)), whereas in NUV BHBs, BSS, RGBs, SGBs and MSs are clearly visible (Fig. 1(b)). We see the main sequence turn-off at 20.3 ABmag in NUV(B4) filter (Fig. 1(b)). We are able to see the MS branch in NUV band which is not visible in the FUV

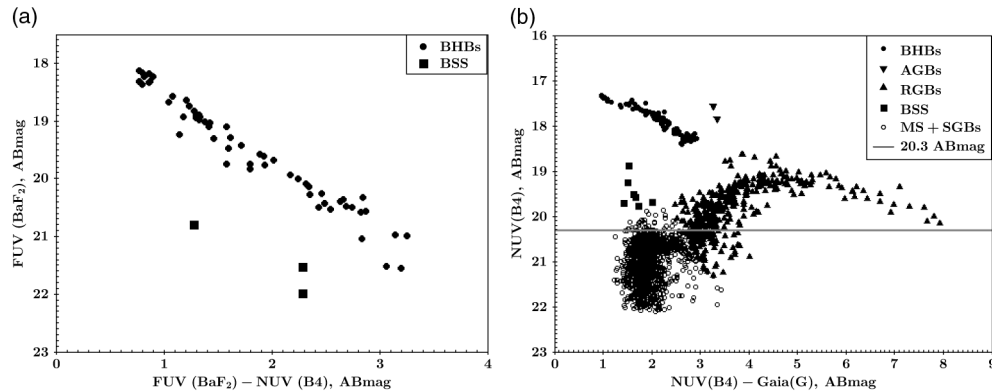


Figure 1. Fig. 1(a) shows the $FUV(BaF_2)$ - $NUV(B4)$ vs $FUV(BaF_2)$ and Fig. 1(b) shows the $NUV(B4)$ - $Gaia(G)$ vs $NUV(B4)$ CMDs of NGC 4590. Various stellar populations present in the cluster are denoted with different symbols: filled circles show the BHBs, filled squares show BSS, lower triangles show AGBs, upper triangles show RGBs, and MS+SGBs are shown with open circles. Gray horizontal line in Fig. 1(b) shows the MS-turn off point in $NUV(B4)$.

band. We have seen a similar trend of distribution of sources in the CMDs of other clusters as well. A list of UV-Bright sources extracted for the four GGCs are given in Table 2.

4. Temperature and Radial Distribution of BHBs and BSS

There have been several studies of temperature distribution of BHBs and BSS of GGCs in UV using GALEX (Schiavon et al. 2012), HST (Lagioia et al. 2015) and UVIT (Sahu et al. 2019) observations. Schiavon et al. (2012); Lagioia et al. (2015) have used zero age horizontal branch (ZAHB) models to extract effective temperature (T_{eff}) from the UV CMDs, whereas Sahu et al. (2019) have used the color-temperature relation from the Kurucz stellar atmosphere model (Castelli & Kurucz 2003) and the SED fitting on the BHBs and BSS sources. In order to extract out T_{eff} of all the observed BHBs and BSS in our observed four GGCs, we have used the color-temperature relation from Kurucz stellar atmosphere model (Castelli & Kurucz 2003). Based on the color combinations used in FUV and NUV CMDs for all the clusters, we generated theoretical colors for a range of temperature (4,000K to 30,000K) using cluster parameters of observed GGCs given in Table 2 and a surface gravity, $\log(g) = 4.0$ for BHBs and BSS (suggested by Lagioia et al. 2015; Sahu et al. 2019, for BHBs). Then observed colors and theoretical colors were matched, within $\sigma_{color} \leqslant 0.01$ which have max $\Delta T = 100K$, to extract the corresponding T_{eff} for each BHB star and BSS. The T_{eff} distribution of 152 BHBs and 42 BSS observed with FUV and NUV filters of UVIT are plotted in Fig. 2. The T_{eff} of BHBs ranges from 8,500K to 17,000K, whereas the T_{eff} of BSS ranges from 9,500K to 12,000K. The temperature distribution shows that there are two groups of BHBs present in the observed GGCs. We also see a gap between 11,500K and 12,000K, which suggests the Grundahl-jump in temperature distribution of BHBs (Grundahl et al. 1999).

We took the core radius, half light radius and the tidal radius from the updated catalogue of GGCs (Harris 2010) and then studied the radial distribution of cluster members observed in FUV and NUV bands. We found that the FUV emissions arise only from the BHBs and BSS sources which are concentrated within half light radius of the clusters. The NUV emissions arise from BHBs, BSS, RGBs and SGBs and their radial distribution goes up to the tidal radius of clusters. A detailed analysis on radial distribution and density of cluster members for all clusters will be done in forthcoming papers.

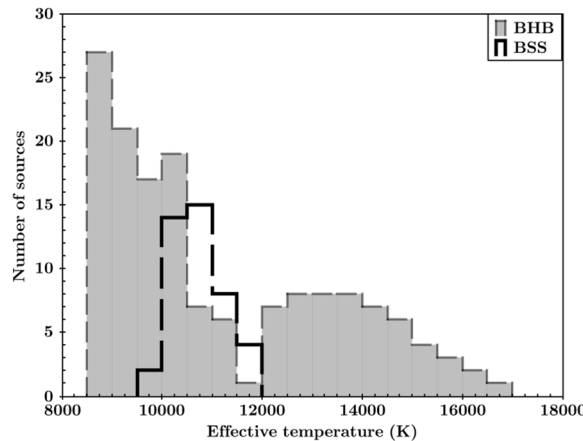


Figure 2. Temperature distribution of BHBs and BSS observed in the four GGCs.

Acknowledgements

This research is supported by ISRO RESPOND PROJECT No. ISRO/RES/2/409/17-18. This publication uses data from the AstroSat mission of the Indian Space Research Organization (ISRO), archived at the Indian Space Science Data Centre (ISSDC).

References

- Ambika, S., Parthasarathy, M., Aoki, W., *et al.* 2004, *A&A*, 417, 293
- Cardelli, J. A., Clayton, G. C., & Mathis, J. S. 1989, *ApJ*, 345, 245
- Castelli, F. & Kurucz, R. L. 2003, *Modelling of Stellar Atmospheres*, A20
- Dalessandro, E., Schiavon, R. P., Rood, R. T., *et al.* 2012, *AJ*, 144, 126
- Dorman, B., O'Connell, R. W., & Rood, R. T. 1995, *ApJ*, 442, 105
- Gaia Collaboration, Brown, A. G. A., Vallenari, A., *et al.* 2018, *A&A*, 616, A1
- Greggio, L. & Renzini, A. 1990, *ApJ*, 364, 35
- Grundahl, F., Catelan, M., Landsman, W. B., Stetson, P. B., & Andersen, M. I. 1999, *ApJ*, 524, 242
- Harris, W. E. 2010, *arXiv e-prints*, arXiv:1012.3224
- Jasniewicz, G., de Laverny, P., Parthasarathy, M., *et al.* 2004, *A&A*, 423, 353
- Lagioia, E. P., Dalessandro, E., Ferraro, F. R., *et al.* 2015, *ApJ*, 800, 52
- Lee, H.-c., Lee, Y.-W., & Gibson, B. K. 2002, *AJ*, 124, 2664
- Milone, A. P., Marino, A. F., Piotto, G., *et al.* 2015, *ApJ*, 808, 51
- Piotto, G., Milone, A. P., Bedin, L. R., *et al.* 2015, *AJ*, 149, 91
- Postma, J. E. & Leahy, D. 2017, *PASP*, 129, 115002
- Rood, R. T., Dorman, B., Ferraro, F. R., Paltrinieri, B., & Fusi Pecci, F. 1998, *Ultraviolet Astrophysics Beyond the IUE Final Archive*, 413, 515
- Sahu, S., Subramaniam, A., Côté, P., Rao, N. K., & Stetson, P. B. 2019, *MNRAS*, 482, 1080
- Schiavon, R. P., Dalessandro, E., Sohn, S. T., *et al.* 2012, *AJ*, 143, 121
- Schlegel, D. J., Finkbeiner, D. P., & Davis, M. 1998, *ApJ*, 500, 525
- Sohn, S. T., O'Connell, R. W., Kundu, A., *et al.* 2006, *AJ*, 131, 866
- Stetson, P. B. 1987, *PASP*, 99, 191
- Subramaniam, A., Sahu, S., Postma, J. E., *et al.* 2017, *AJ*, 154, 233
- Tandon, S. N., Subramaniam, A., Girish, V., *et al.* 2017, *AJ*, 154, 128